Scientific Papers Series Management, Economic Engineering in Agriculture and Rural Development
Vol. 23, Issue 1, 2023
PRINT ISSN 2284-7995, E-ISSN 2285-3952

3D PRINTING TECHNOLOGY AS AN EFFECTIVE SOLUTION TO BUILD THE FABA BEAN SEED METER PLATE WITH VARIOUS MATERIALS

Tarek FOUDA[1], Abeer ABDELSALAM[1], Atef SWILAM[2], Mohamed El DIDAMONY[1]

[1]Tanta University, Faculty of Agriculture, Agriculture Engineering Department, Egypt
Phone:+201000350643, Fax:0020403455570, E-mails: tfouda628@gmail.com, abeergmal1369@gmail, agri.mid@gmail.com
[2]International Center for Agricultural Research in the Dry Areas (ICARDA), Cairo, Egypt
Currently: Office of Innovation, UN-FAO, Rome, Italy, Email: Atef.swelam@fao.org

Corresponding author: tfouda628@gmail.com

Abstract

The difference in some dimensions of the seeds prevents the optimal determination of the dimensions and shape of the holes in the feeding device, which reduces the efficiency of seed distribution during planting. The design and building of metering plates suitable for the faba bean seeds from material that is affordable and appropriate for the environmental and operational conditions during their onset on the land to cultivate the crop and enhance productivity. The plates were built by 3D printing by Tanta Motors - Egypt and tested at the Department of Agricultural Engineering - Faculty of Agriculture, Egypt. This research study was conducted for the design and development of plates. The discs were designed and built through a series of processes that were defined and plotted in proportion to the main dimensions and shape index of the seed. The materials analysis was tested by (Solidworks). Changes in materials (Acrylonitrile butadiene styrene- Polyamide Nylon and Thermoplastic polyurethane) and shape index 1.7674 and 1.8782 were tested at Stress, displacement, Strain analysis, mesh, Deformation, and plate safety factor. Moreover, the simulation results indicated that the computational values were in agreement with the theoretical values. They all showed that the model and boundary conditions were correct and logical, and would provide a scientific basis for the optimal design.

Key words: *metering plate, seed planting, solid works, 3D printer, 3D max*

INTRODUCTION

Since the 19th century, the lateral shape of some seeds has been described as reniform, which is derived from the Latin rein, kidney, so reniform means kidney-shaped. Kidneys, on the other hand, are not geometric shapes, their shape is not well defined. Thus, the term "kidney" corresponds to descriptive rather than analytical language. On the other hand, seeds are similar to cardioid curves, and the expression "cardioid curve" belongs to the language of analysis because it defines a graph with the precision of an algebraic equation, allowing the graph to be explicitly represented and the similarity quantified in different images to which it resembles. The shapes of seeds of different species are explained by comparing them to geometric models [13], [15].

Seed morphological variety includes variations in terms of seed size and shape. The form of the seed is the most important factor in plant identification and categorization. It is particularly important in agriculture since it represents genetic, physiological, and ecological components, all of which have an impact on production, quality, and market price. The advancement of quantification and modelling methodologies, as well as the application of digital technologies, allows for a more precise description of seed morphology.
Image processing technologies are being used to estimate seed size and morphology automatically. Shape quantification methods are mainly based on these models and are essential for an appropriate depiction, allowing for comparison across polymorphisms or developmental phases, as

well as calculating the degree of variation in specific types of seeds [3].

Shape quantification techniques usually on these models are crucial for an accurate reflection, allowing for comparison across polymorphisms or developmental phases, as well as calculating the degree of variation in specific types of seeds [6].

The results of seed morphology are important in systematics because they help with genotype differentiation. Seed size and shape measurements, as well as their connection and interaction, are crucial in seed yield breeding [1].

Understanding the relationship between seed form and agronomic factors may help enhance yield or quality [24].

Computer-aided image analysis systems can examine morphological seed characteristics, and data may be swiftly processed and saved on a hard disc, displayed, or statistically elaborated. Digital imaging may be a quick and dependable tool for a wide range of discrimination [5].

Although seed shape is a significant characteristic in the phenotypic description as well as plant identification and categorization, its usage in plant science and agronomy requires measurement. Accurate seed shape estimation may give new data in morphology and taxonomy. Furthermore, seed form is the end product of genetic, physiological, and environmental variables, and it influences quality and market price. Thus, quantifying seed shape is of interest in many aspects of plant science and is also important in agriculture [4].

A recent study of several approaches for seed shape estimation based on the comparison of seed photos with geometric shapes was published. Geometric figure modelling contributes to enhanced precision in seed equations to describe, permitting for the discovery of morphological variation such as variations in imbibition, mutations, variances among related genotypes, or shape changes in response to environmental influences [12].

The appearance of seeds is a crucial factor in differentiating them. The form of the seeds is easy to discern, and shape is a convenient and cost-effective technique to examine the seed. Seed shape and size are essential aesthetic characteristics for determining diversity and quality. The form is also employed in classification, breeding, and the design of equipment. Identifying such characteristics will also help in the drying, storing, packing, and shipping operations. Furthermore, form, size, area, and mass-like physical characteristics are employed in a variety of critical operations such as processing, dehulling, cleaning, and separation [2].

Grain seeders are essential pieces of field planting technology. The seed meter is an essential component of the planter. The effect's quality will have a direct impact on the cost and quality of crop planting and post-workload. Precision seed metering devices are classified into mechanical and pneumatic types based on their operating principles. The pneumatic seed metre is highly adaptable to seeds, has low light damage, and so on, but its construction is complex, and its cost and technical requirements are high [21].

There are several techniques for planting seeds, including seedling transplantation, manual broadcasting, and direct sowing. The planting pattern is the most traditional planting method, which is arduous, time consuming, and expensive, as well as broadcast and rigorous in environmental conditions. As a result, these parameters must be satisfied in order to avoid unequal distribution and low output [9].

all precision seed meters built on the idea of seed singulation have seed miss issues. focuses on identifying methods and exploring the potential for eliminating seed misses. Modelling single and double miss provided evidence for the proposed method's potential [17].

a mechanism that releases just one seed at a time is the seed metering device of a precision seeder. The majority of the seed metering equipment in use today uses a revolving metering mechanism to singulate and measure the seeds. There may likely be an accuracy issue while handling singulation and uneven seed shape [25].

precision seeding technology has become a widely used seeding technology in the process of agricultural development to increase

PRINT ISSN 2284-7995, E-ISSN 2285-3952

efficiency and get higher economic benefits. Future agricultural progress will focus heavily on the high-speed and small-spacing sowing method [26].

SolidWorks is the industry standard for 3D solid modeling, automated design, engineering analysis, and product preparation for any complexity and purpose. Depending on the type of work to be solved, three main system configurations are available: Solid Works Standard, Professional, and Premium are the three editions of Solid Works [14].

The polymers Acrylonitrile-Butadiene-Styrene are made up of three monomer units: Acrylonitrile, Butadiene, and Styrene. Plastic has numerous adaptable features such as heat resistance, light weight, easy formability, reflectivity, and so forth [23].

3D printing technology is a type of rapid prototyping technology, also known as additive manufacturing technology. It is a type of technology based on digital model files, using adhesive materials such as polymer materials or metal powder to construct objects by printing layer by layer. On a computer, the 3D model is simulated and sliced to decompose it into a multi-layer 2D structure. The printing consumables are then fused at high temperatures before being extruded layer by layer through a nozzle. Finally, a 3D structure that is identical to the design model is created. Polymers have attracted a lot of attention because they cannot only be formed quickly but also have good mechanical strength and functionality. The most common polymer is acrylonitrile butadiene styrene copolymer (ABS), which is one of the most widely used polymers with the highest output at the moment. It has heat resistance, impact resistance, low-temperature resistance, chemical corrosion resistance, excellent electrical performance, and consistent product size. Its application range includes almost all daily necessities as well as engineering supplies [28], [8], [27], [11].

Nylon, ASA, PLA, TPU, PMMA, and PETG are common polymers used in product preparation [20].

This study designed and evaluated modern metering plates for faba bean seeds that needed simple movement for seeds that are crucially moving during metering plate filling. The primary goal of this study is to discover the form shape index and the optimal material for manufacturing of faba bean discs that are both environmentally and operationally acceptable.

MATERIALS AND METHODS

Design of the faba bean plates

The plates were designed in solid works software with version 2018, and manufactured by the 3D printer and the realistic 3D model of the faba bean was designed in 3D max software with version 2017 as shown in Figures (1 - 6).

Solidworks Analysis

The model was analyzed by the 2018 version of Solidworks software. Used to analyze the material properties of discs to determine materials that are compatible with environmental and operational impacts during planting operations.

The static simulation steps of exposure mainly include:

(1) Create 3D geometric models and meshes
(2) Define the material of the model
(3) Identify fixtures parts
(4) Define the external load
(5) Define the contact surface

Material Data

1-ABS (Acrylonitrile butadiene styrene)

Table 1. Material properties of ABS

Item	*Value*
► elastic modulus	► 2,000 N/mm^2
► poison's ratio	► 0.394N/A
► shear modulus	► 318.9N/mm^2
► mass density	► 1,020Kg/m^3
► tensile strength	► 30N/mm^2
► thermal conductivity	► 0.2256W/M.K
► specific heat	► 1,386 J/Kg.K

Source: Own results.

2-PA (Polyamide Nylon)

Table 2. Material properties of PA

Item	*Value*
► elastic modulus	► 2,620 N/mm^2
► poison's ratio	► 0.34N/A
► shear modulus	► 970.4N/mm^2
► mass density	► 1,120Kg/m^3
► tensile strength	► 90N/mm^2
► thermal conductivity	► 0.233W/M.K
► specific heat	► 1,601J/Kg.K

Source: Own results

3-TPU (Thermoplastic polyurethane)

Table 3. Material properties of TPU

Item	***Value***
elastic modulus	0.621GPa
Flexural Modulus	4.50 GPa
Hardness	70
mass density	1,225 Kg/m^3
tensile strength	28.0-96.0MPa

Source: Own results.

Table 4. Equations used to calculate the size and shape attributes and analysis

Variables	Equations*	Literature
Elongation (E)	$E = \frac{L}{W}$	Fıratlıgil-Durmuş et al. (2010) [7]
Projected area(A)	$A = \frac{\pi}{4} \times (Dg)^2$	Afonso Junior et al. (2007)[10]
Roundness(R)	$R = \frac{(4 \times Area)}{\pi \times (L)^2}$	Sayinci et al. (2015)[18]
Flatness Index(FI)	$FI = \frac{(L+W)}{(2 \times TH)}$	Cervantes et al(2016)[3]
Shape Index(SI)	$SI = \frac{2 \times L}{W+TH}$	Ozkan and Koyuncu (2005) [16]
Geometric Mean Diameter (DG),mm	$Dg = (WLT)^{\frac{1}{3}}$	Ozkan and Koyuncu (2005) [16]
ESTREN	$ESTRN = 2[\frac{(\varepsilon 1+\varepsilon 2)}{3}]^{\frac{1}{2}}$ $\varepsilon 1 = 0.5[(EPSX - \varepsilon^*)2 + (EPSY - \varepsilon^*)2 + (EPSZ - \varepsilon^*)2]$ $\varepsilon 2 = \frac{[(GMXY)2 + (GMXZ)2 + (GMYZ)2]}{4}$ $\varepsilon^* = \frac{(EPSX + EPSY + EPSZ)}{3}$	Segalman et al(2000)[19]
von Mises	$V.Mises = \{\frac{[(\sigma 1-\sigma 2)^2+(\sigma 2-\sigma 3)^2+(\sigma 1-\sigma 3)^2]}{2}\}^{\frac{1}{2}}$	Segalman et al(2000)[19]
URES	$URES = \sqrt{X^2 + Y^2}$	Simo et al(1989)[22]

L= Length, mm, W= Width, mm, TH= Thickness, mm, Dg= Geometric Mean Diameter, mm, ε 1=Normal strain in the first principal direction. ε 2=Normal strain in the second principal direction. ε 3=Normal strain in the third principal direction. EPSX, EPSY, and EPSZ =Normal strain in the X, Y, and Z direction of the selected reference geometry.GMXY=Shear strain in the Y direction in the YZ-plane of the selected reference geometry. GMXZ=Shear strain in the Z direction in the YZ-plane of the selected reference geometry. GMYZ=Shear strain in the Z direction in the XZ-plane of the selected reference geometry.$\sigma 1 \backslash \sigma 2 \backslash \sigma 3$=principal stresses. X=is the first direction that the object is traveling. Y=s the second direction that the object is traveling
Source: Authors' determination.

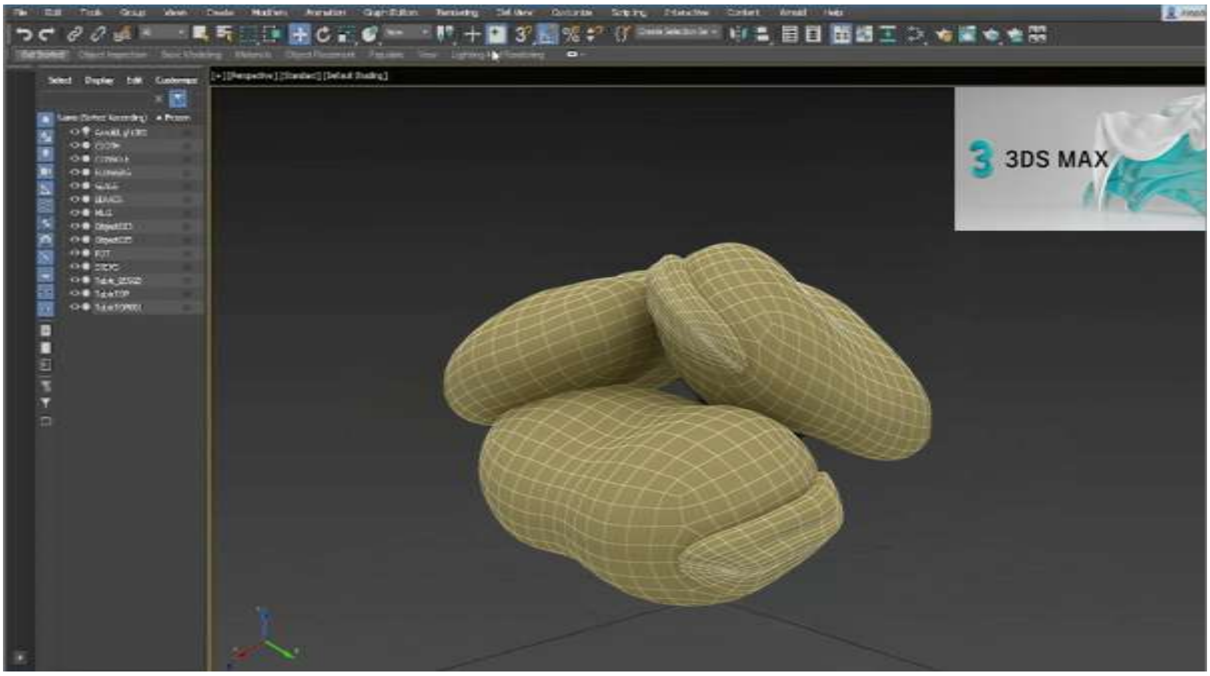

Fig. 1. Faba Bean Seeds with 3D max software
Source: Authors' determination.

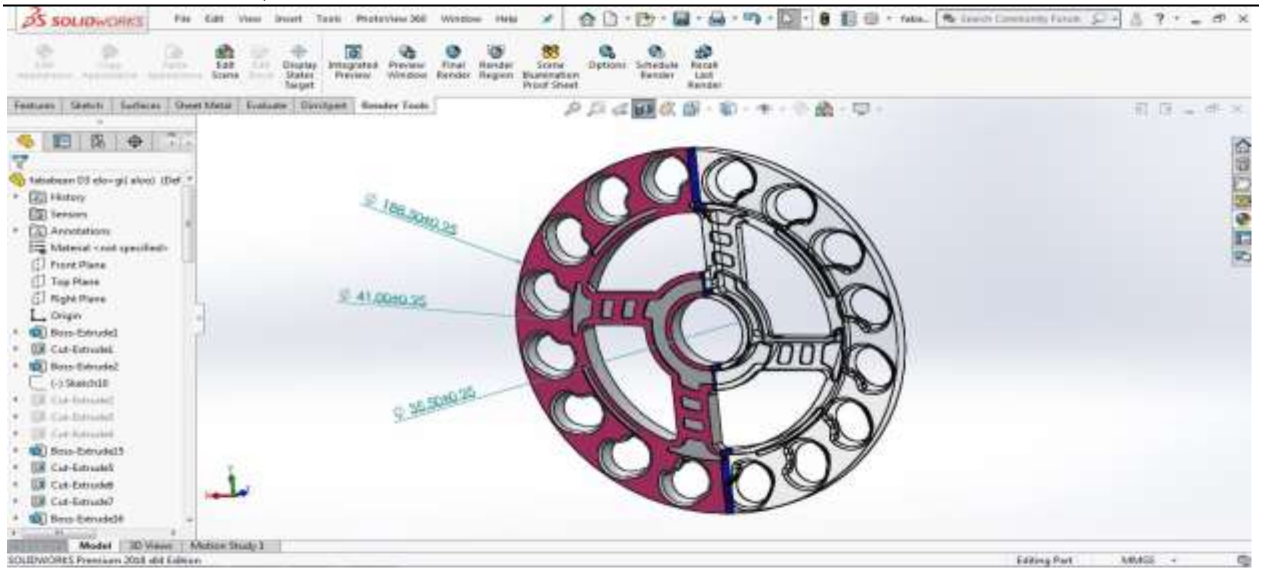

Fig. 2. Design of faba bean plate with Solidworks Software (V.2018)
Source: Authors' determination.

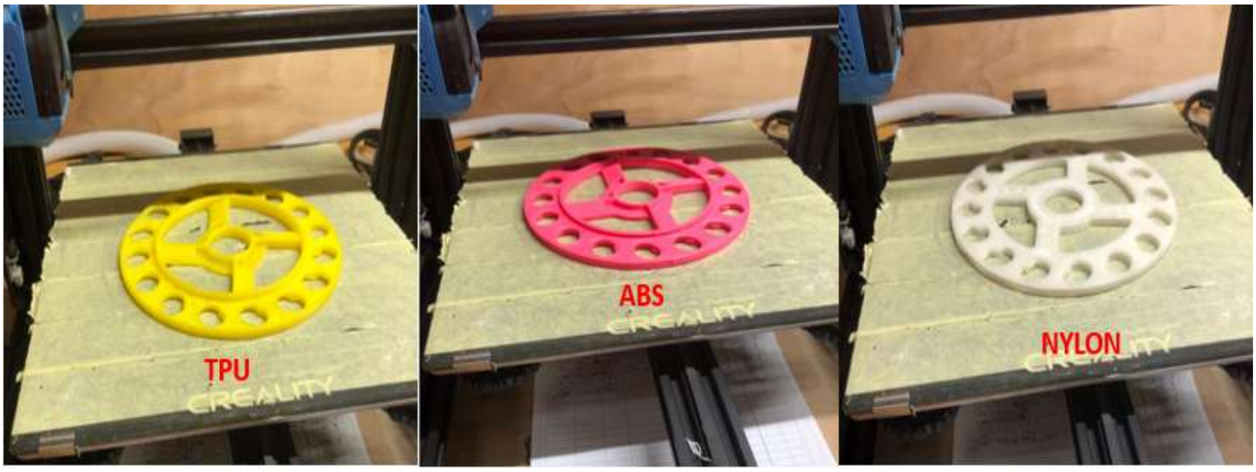

Fig. 3. Metering Plates of Faba Bean with 3D Printer in Final Stage for (TPU-ABS-NYLON) material
Source: Authors' determination.

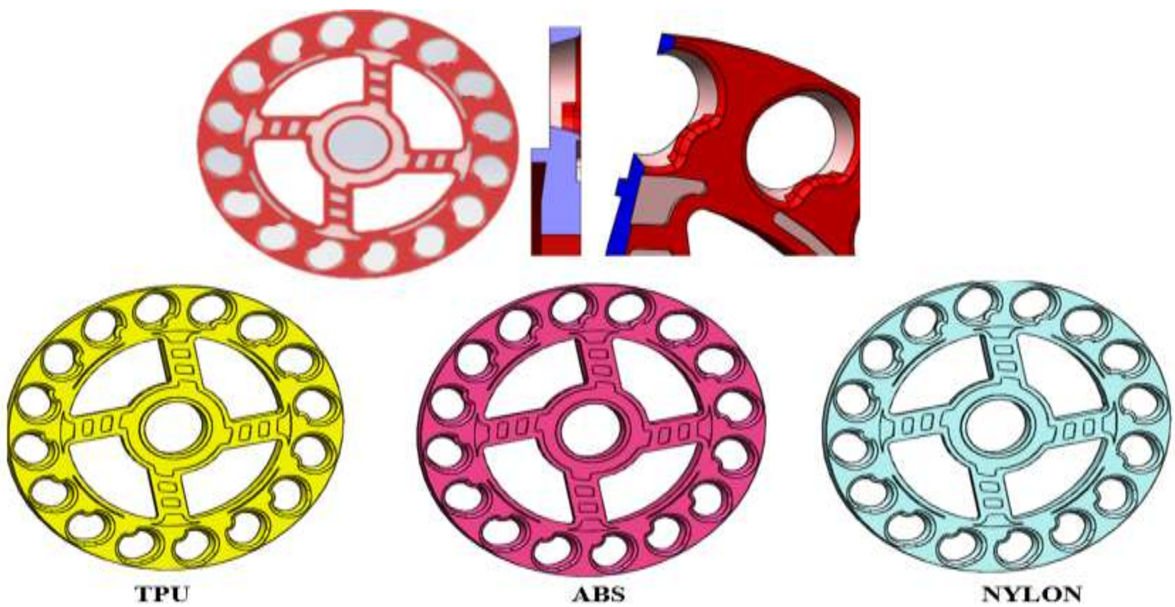

Fig. 4. The Plate 1 of metering discs of faba bean seeds with 3 materials
Source: Authors' determination.

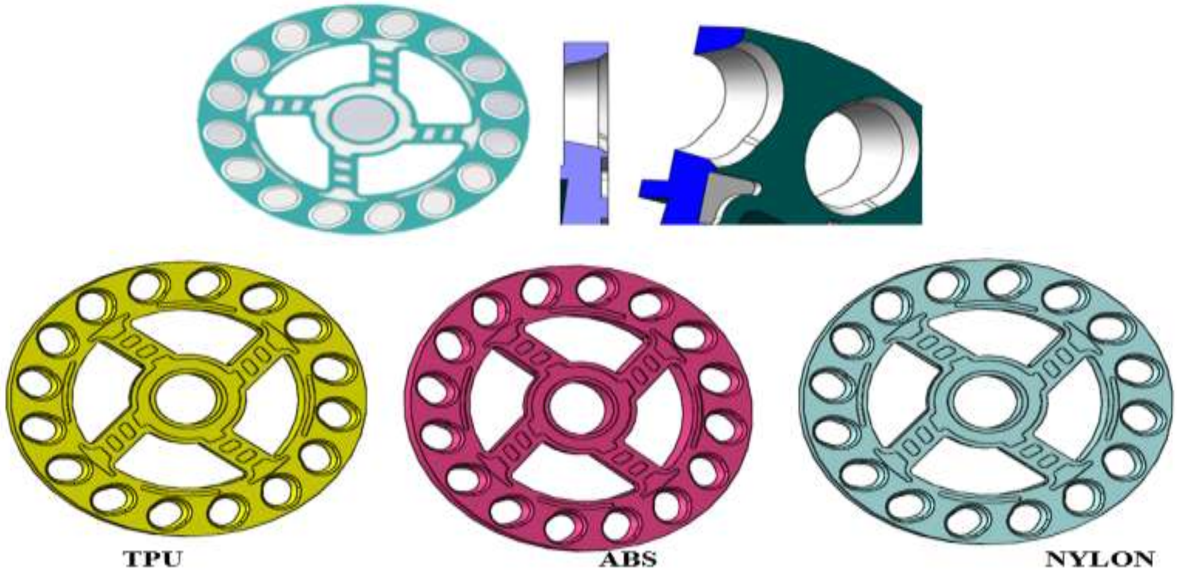

Fig. 5. The Plate 2 of metering discs of faba bean seeds with 3 materials
Source: Authors' determination.

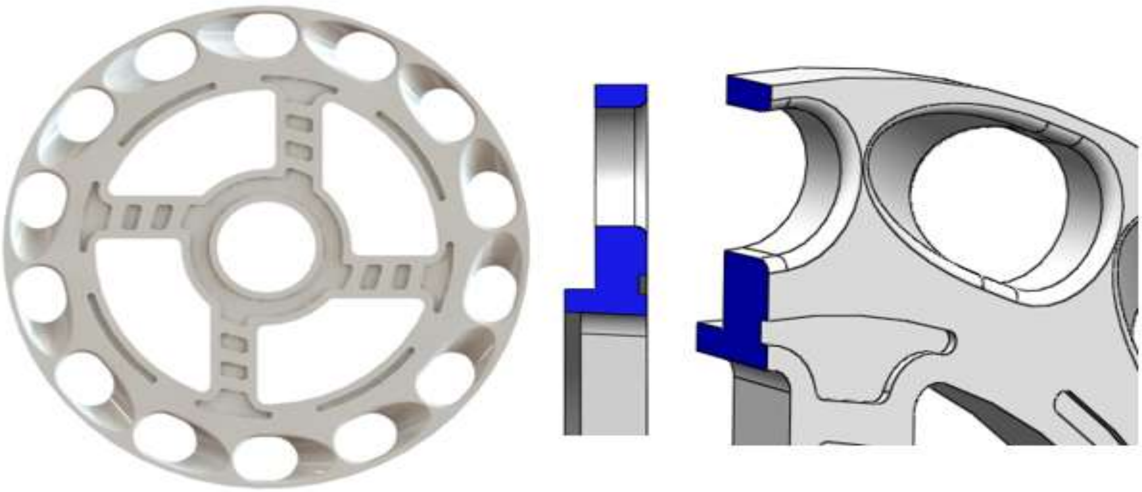

Fig. 6. The Plate 3 of metering discs of faba bean seeds with (PA) material
Source: Authors' determination.

RESULTS AND DISCUSSIONS

The Faba bean form index was evaluated and statistically examined.

Figures demonstrate the link between the shape index of seeds and the shape index of discs as investigated using Solidworks simulation (7- 39).

Shape Index of Faba Bean Seeds

The results showed the average elongation, projected area, flatness, and roundness and shape index, Geometric Mean Diameter of faba bean seeds were (1.356,107.54, 2.04, 0.743 and 1.705) respectively.

The results showed the average elongation, projected area, flatness, and roundness. shape index, Geometric Mean Diameter of the disc (plate 1) were (1.26, 117.81, 2.61, 0.789, 1.76, and 12.25) respectively.

The results showed the average elongation, projected area, flatness, and roundness. and shape index, Geometric Mean Diameter of the disc (plate 2) were (1.23, 136.88, 2.92, 0.809, 1.787, and 13.20) respectively.

The results showed the average elongation, projected area, flatness, and roundness. Shape index, Geometric Mean Diameter of the disc (plate 3) were (2.08, 194.06, 4.036, 0.479, 3.018, and 15.723) respectively.

Table 5. Plates Analysis Results

MATERIAL	PLATE	ANALYSIS		VALUE
ABS	P1	Mesh		103,272
		Stress	Max	1.919e+04 N/m^2
			Min	7.162e-03 N/m^2
		Displacement		4.202e-04 mm
		Strain	Max	4.620e-06
			Min	5.710e-10
	P2	Mesh		31,137
		Stress	Max	1.537e+03 N/m^2
			Min	1.738e-01 N/m^2
		Displacement		4.425e-05 mm
		Strain	Max	3.778e-07
			Min	7.178e-11
TPU	P1	Mesh		103,272
		Stress	Max	1.600e+04 N/m^2
			Min	1.572e-02 N/m^2
		Displacement		1.596e-01 mm
		Strain	Max	1.929e-03
			Min	3.109e-07
		FOS	Max	5.874e+08
			Min	5.775e+02
	P2	Mesh		31,137
		Stress	Max	1.436e+03 N/m^2
			Min	1.148e-01 N/m^2
		Displacement		1.643e-02 mm
		Strain	Max	1.521e-04
			Min	5.397e-08
		FOS	Max	8.045e+07
			Min	6.432e+03
PA	P3	Mesh		31,993
		Stress	Max	9.176e+02 N/m^2
			Min	1.385e-01 N/m^2
		Displacement		2.846e-05 mm
		Strain	Max	2.380e-07
			Min	5.997e-11
		FOS	Max	7.482e+08
			Min	1.130e+05

Source: Authors' determination.

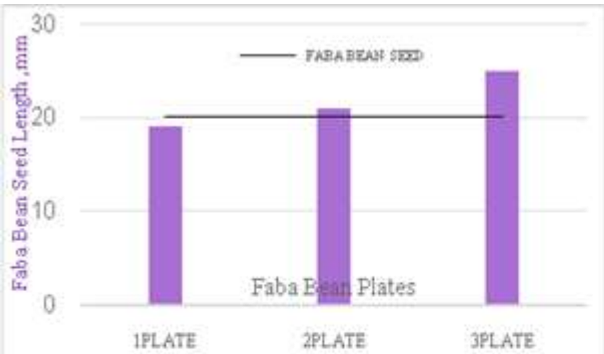

Fig. 7. The relationship between the length of faba bean seeds and the length of holes in various metering plates
Source: Authors' determination.

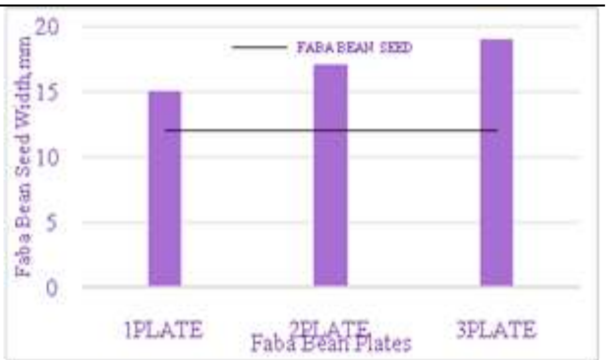

Fig. 8. The relation between faba bean seed width and hole width in various metering plates Source: Authors' determination.

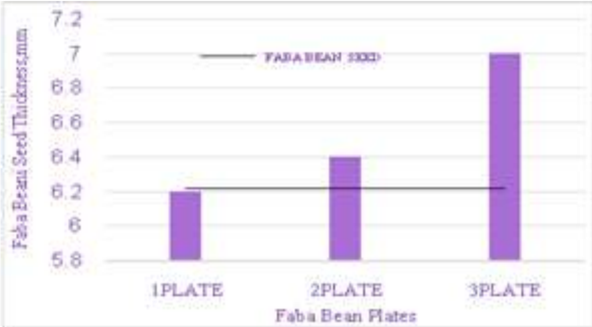

Fig. 9. The thickness of faba bean seeds in proportion to the thickness of holes in various metering plates
Source: Authors' determination.

Fig. 10. The relationship between the elongation of faba bean seeds and the elongation of holes in various metering plates
Source: Authors' determination.

Fig. 11. The relation of flatness index of faba bean seeds and the holes in various metering plates
Source: Authors' determination.

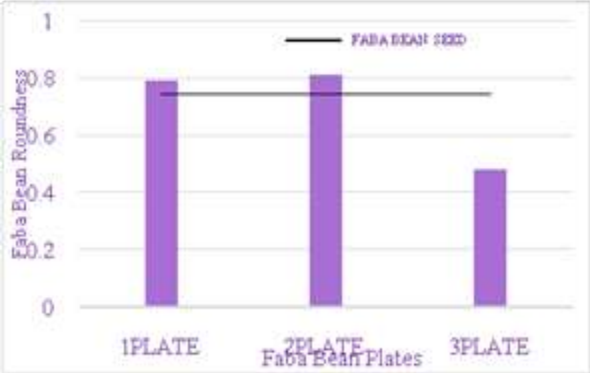

Fig. 12. The relationship between the roundness of holes in various metering plates , faba bean seeds
Source: Authors' determination.

Fig. 13. The relation between faba bean seeds and the holes in various metering plates of the projected area
Source: Authors' determination.

Fig. 14. The relationship between the Geometric Mean Diameter of faba bean seeds holes in various metering plates.
Source: Authors' determination.

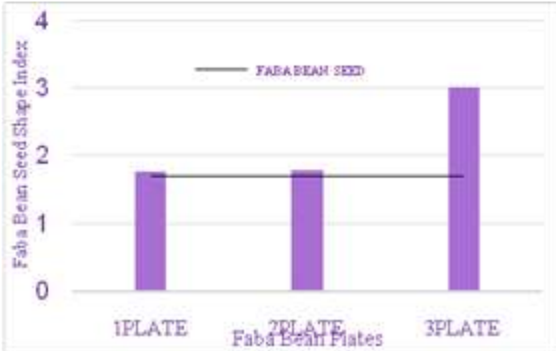

Fig. 15. The relation between the shape index of faba bean seeds and the holes in various metering plates
Source: Authors' determination.

❖ Faba Bean plates (Plate 1)

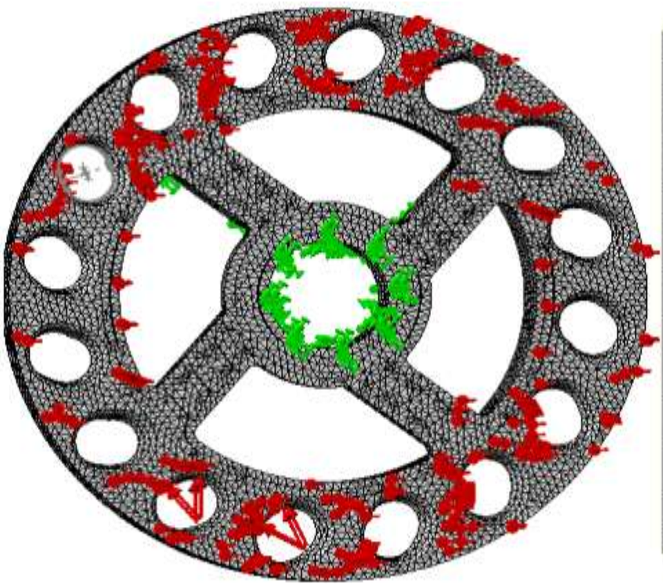

Study name	Static 2 (-Default-)
Mesh type	Solid Mesh
Mesher Used	Standard mesh
Automatic Transition	Off
Include Mesh Auto Loops	Off
Jacobian points	4 points
Element size	2.41547 mm
Tolerance	0.120773 mm
Mesh quality	High
Total nodes	103272
Total elements	61910
Maximum Aspect Ratio	17453
Percentage of elements with Aspect Ratio < 3	98
Percentage of elements with Aspect Ratio > 10	0.111
% of distorted elements (Jacobian)	0
Time to complete mesh(hh:mm:ss)	00:00:20
Computer name	DELL-PC

Fig. 16. Mesh generation of plate 1 (Total number of nodes103272).
Source: Authors' determination.

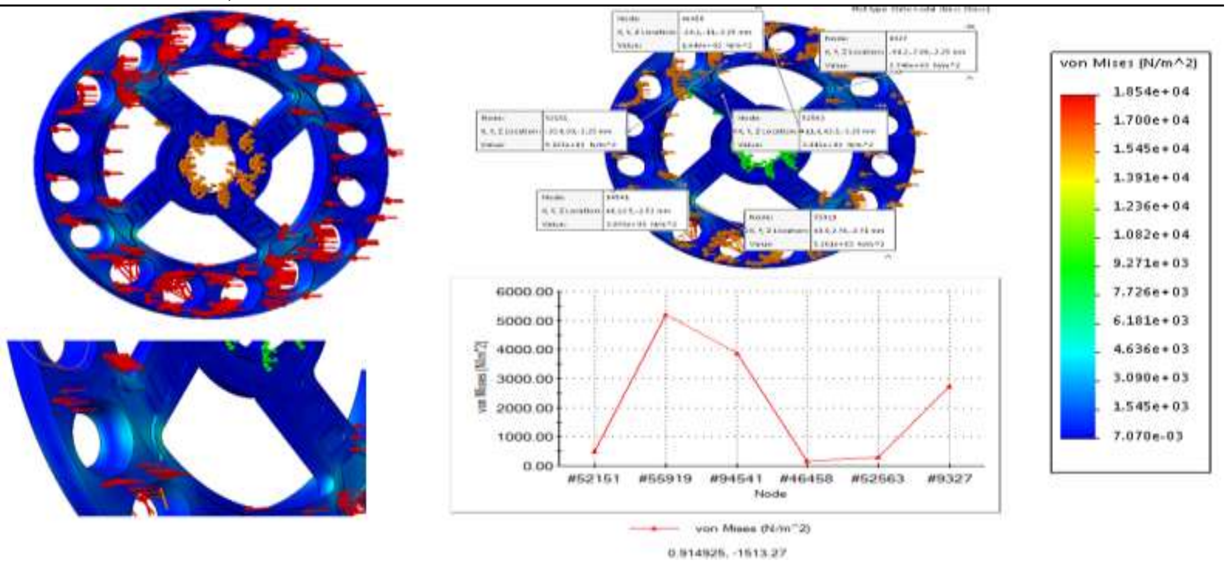

Fig. 17. Stress of the plate 1 of metering plates of faba bean seeds with (ABS) material.
Source: Authors' determination.

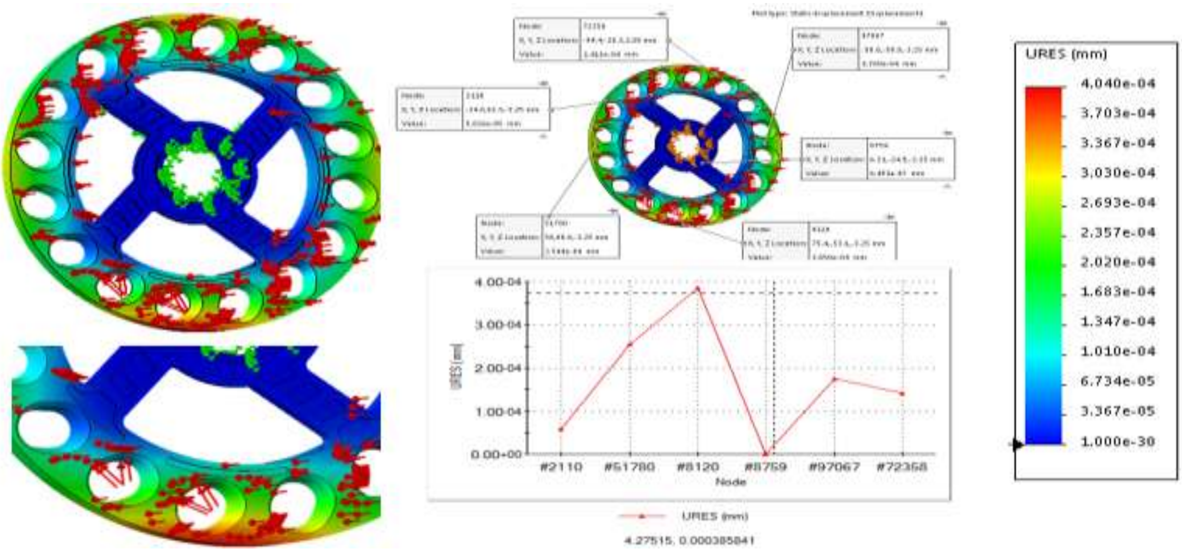

Fig. 18. Displacement of the plate 1 of metering plates of faba bean seeds with (ABS) material.
Source: Authors' determination.

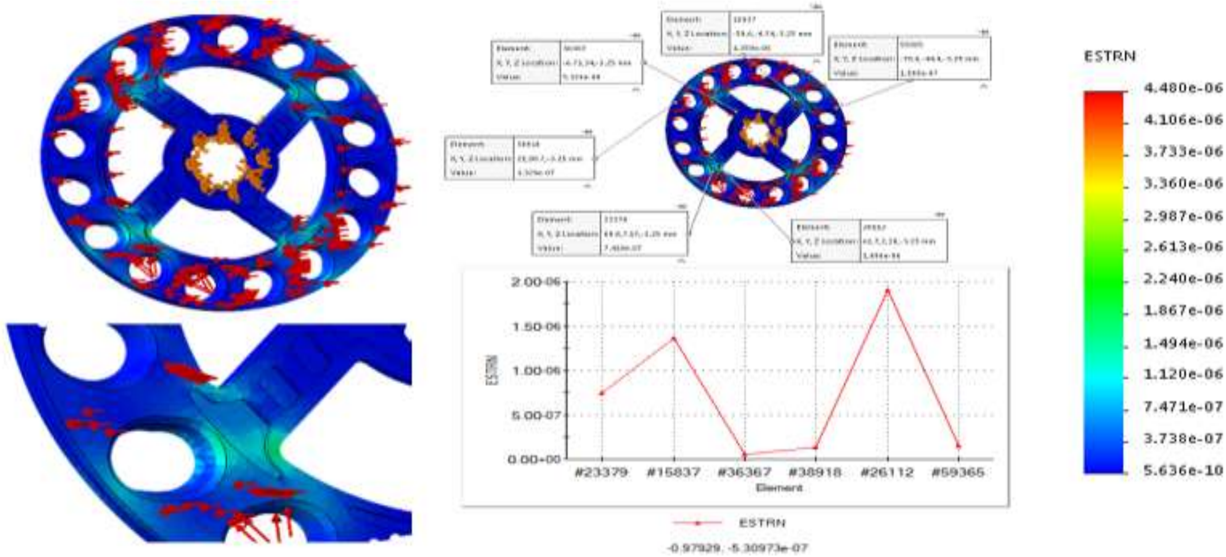

Fig. 19. Strain of the plate1 of meteringplates of faba bean seeds with (ABS) material.
Source: Authors' determination.

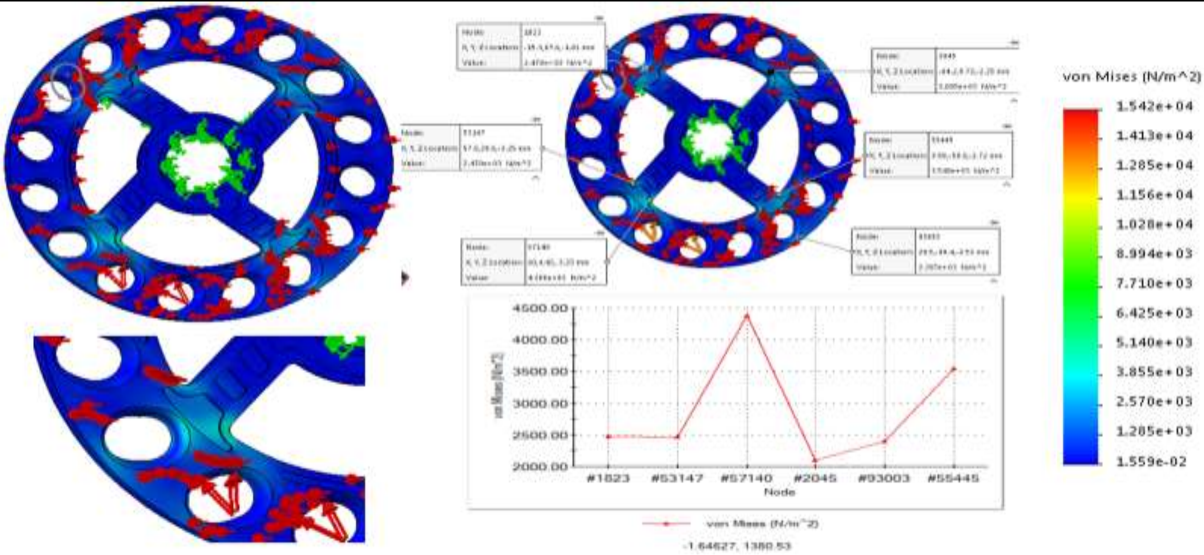

Fig. 20. Stress of the plate 1 of metering plates of faba bean seeds with (TPU) material.
Source: Authors' determination.

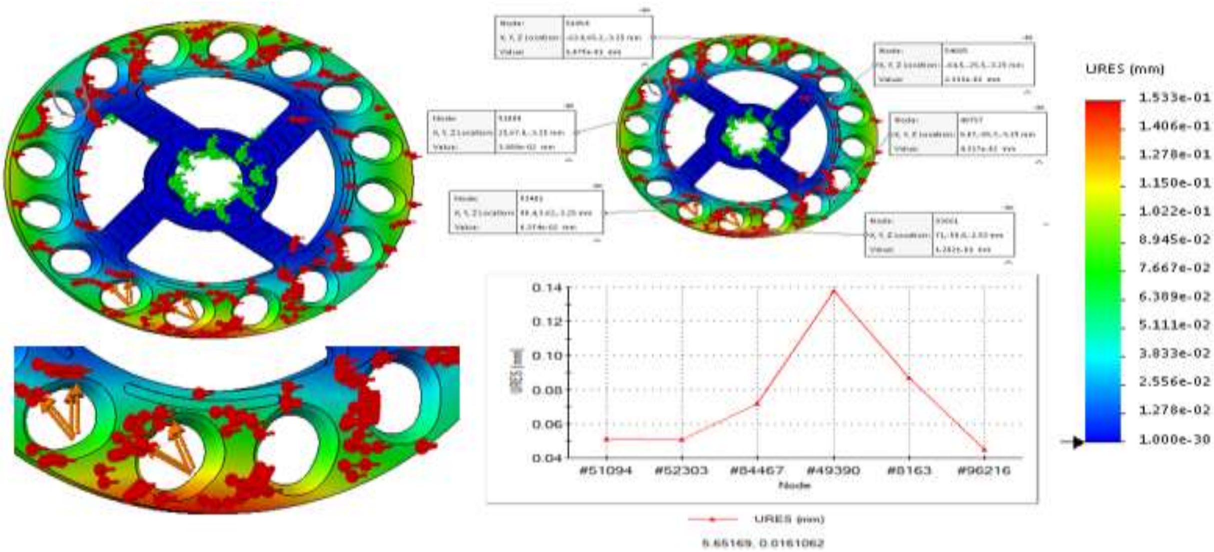

Fig. 21. Displacement of the plate 1 of metering plates of faba bean seeds with (TPU) material.
Source: Authors' determination.

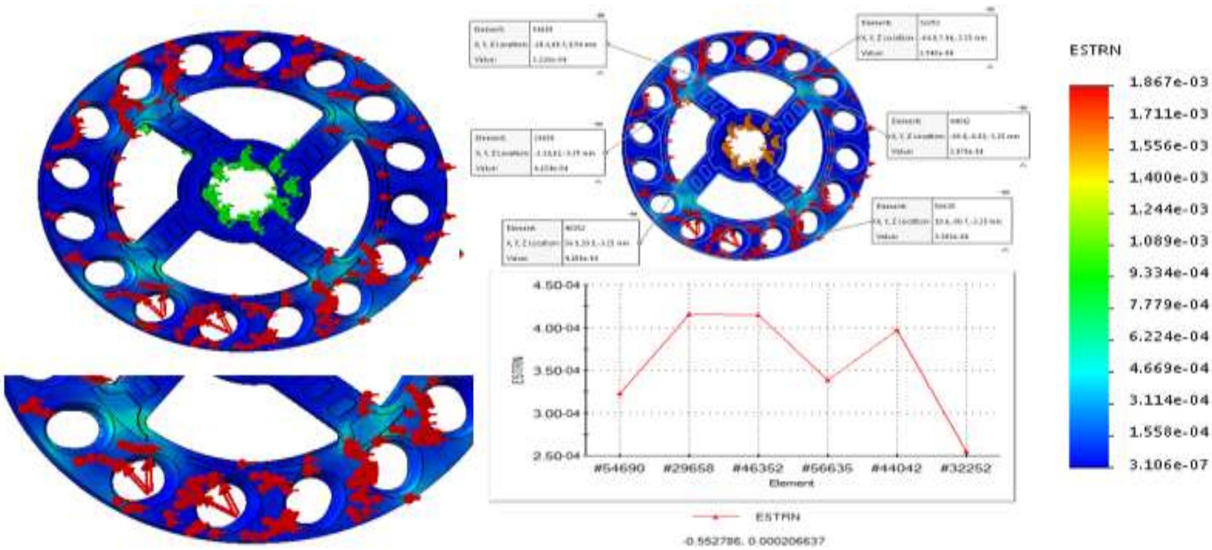

Fig. 22. Strain of the plate 1 of metering plates of faba bean seeds with (TPU) material
Source: Authors' determination.

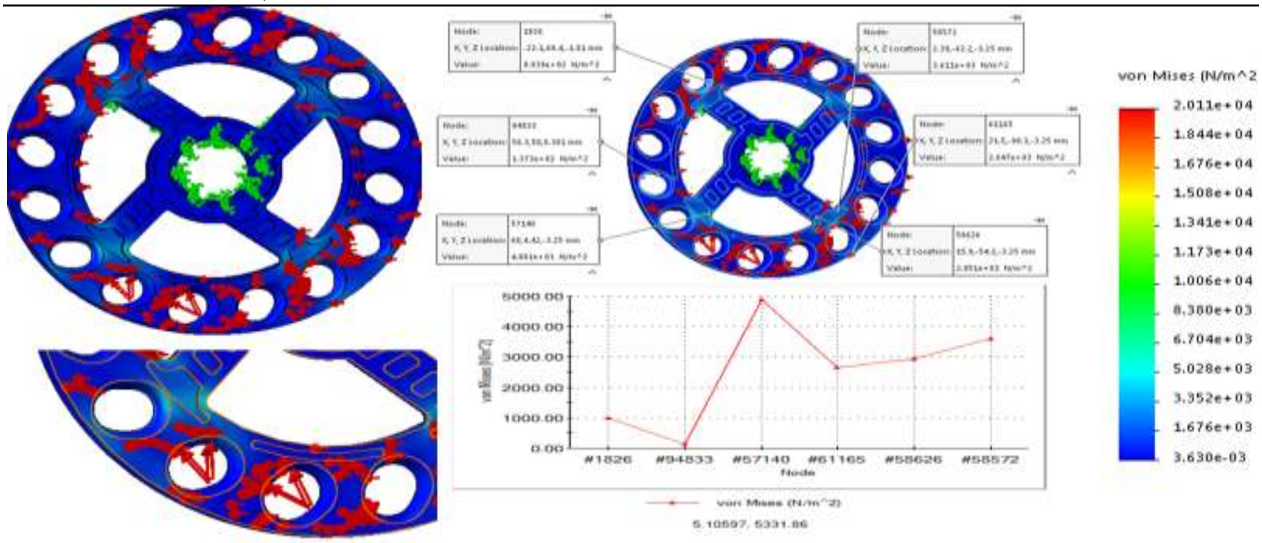

Fig. 23. Stress of the plate 1 of metering plates of faba bean seeds with (NYLON) material.
Source: Authors' determination.

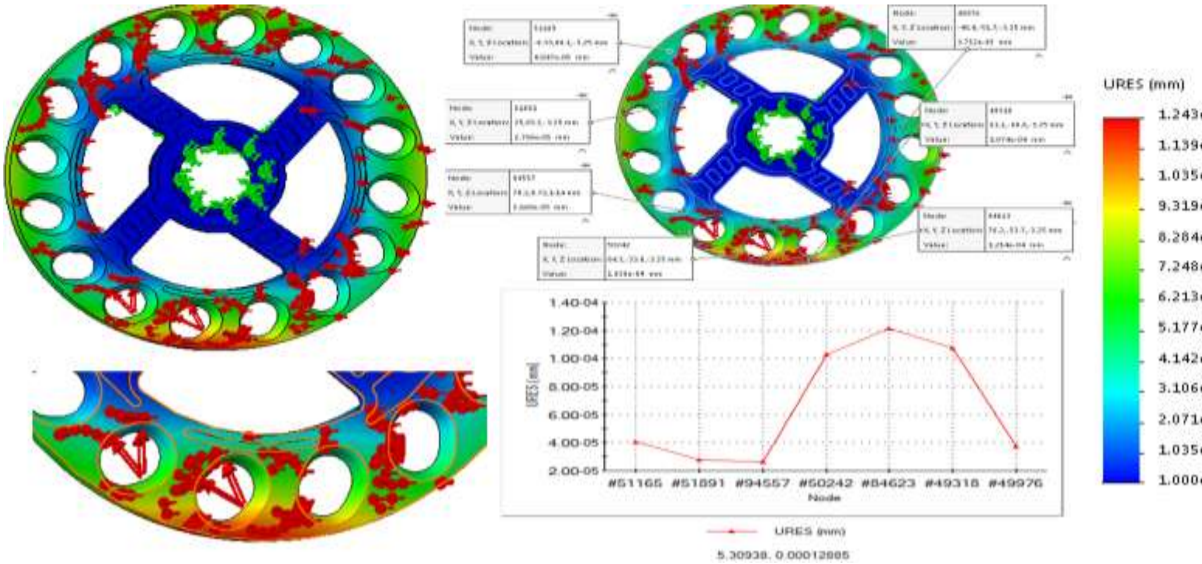

Fig. 24. Displacement of the plate 1 of metering discs of faba bean seeds with (NYLON) material
Source: Authors' determination.

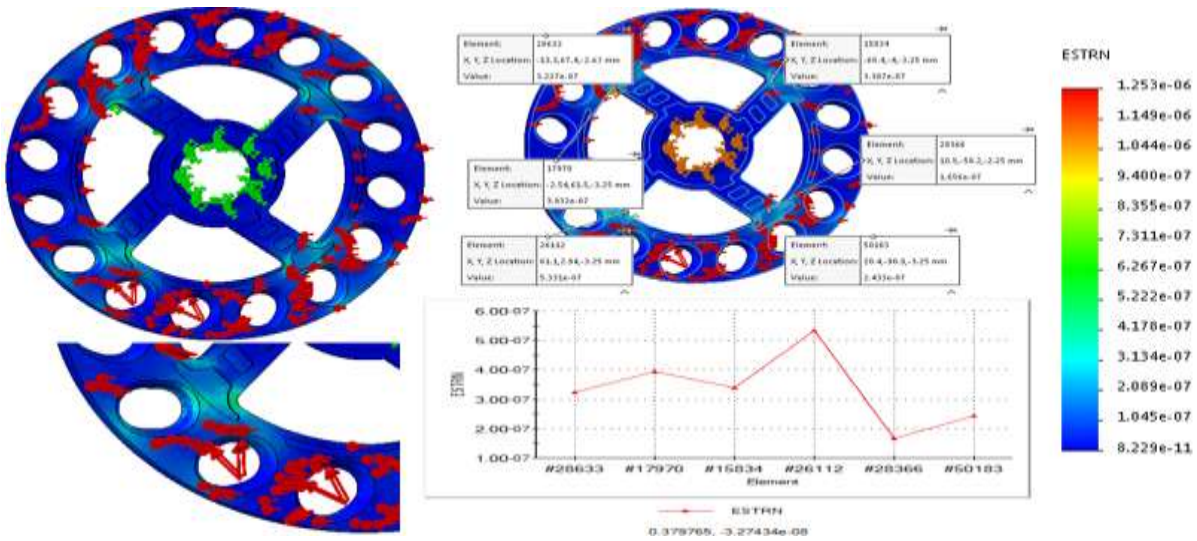

Fig. 25. Strain of the plate 1 of metering plates of faba bean seeds with (NYLON) material.
Source: Authors' determination.

❖ Faba Bean plates (Plate 2)

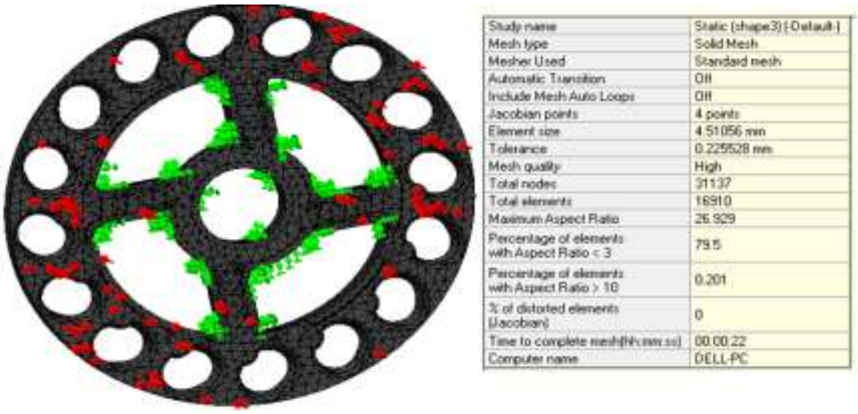

Fig. 26. Mesh generation of plate 2 (Total number of nodes 31137)
Source: Authors' determination.

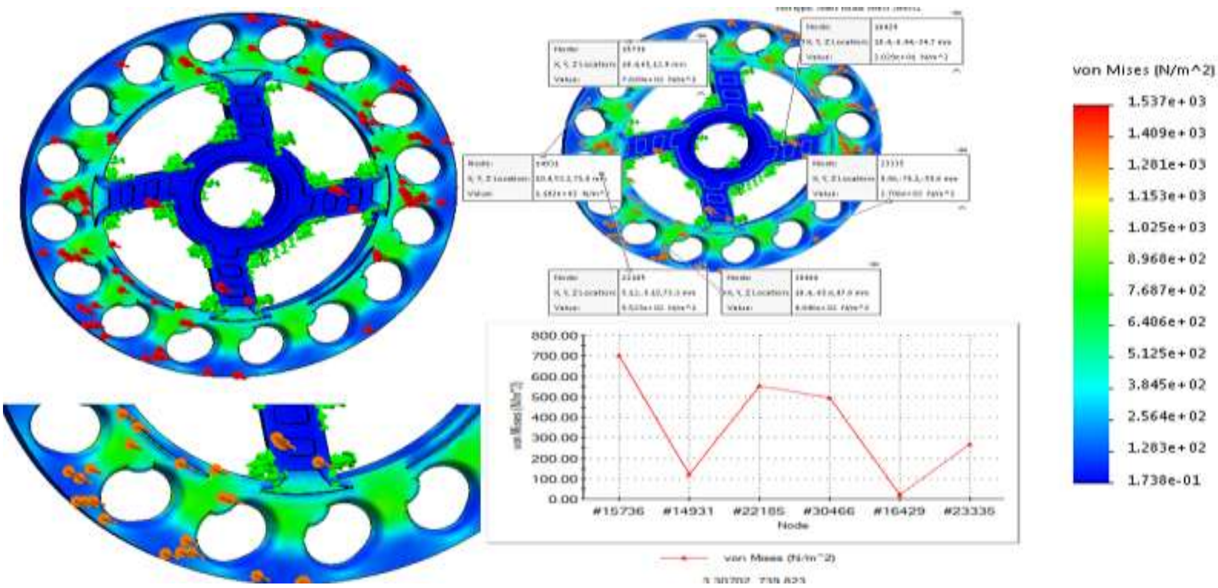

Fig. 27. Stress of the plate 2 of metering plates of faba bean seeds with (ABS) material
Source: Authors' determination.

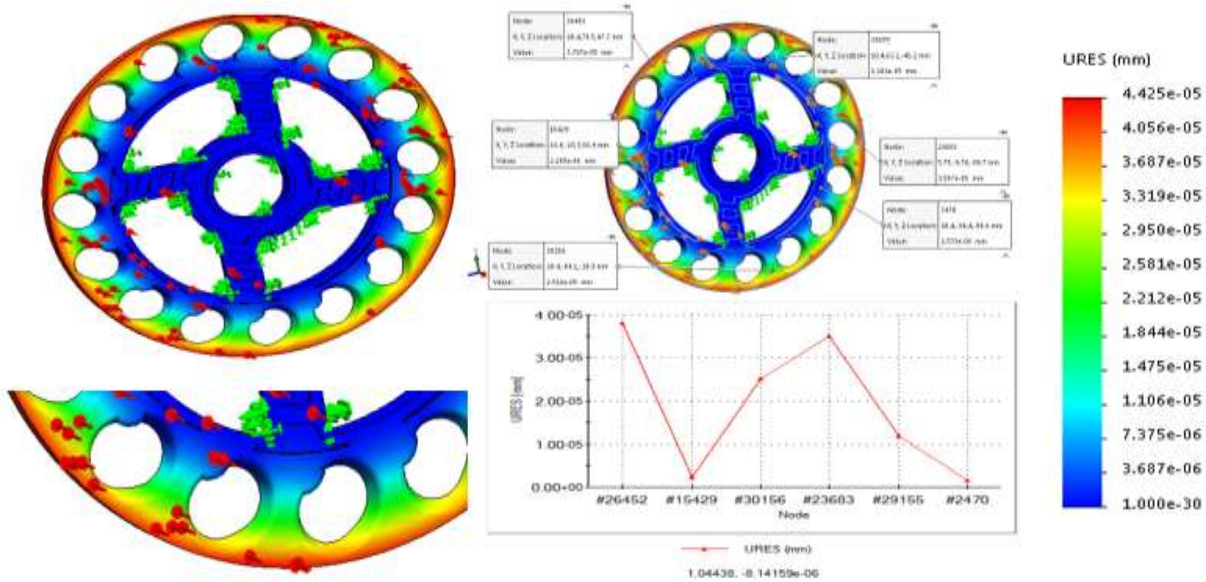

Fig. 28. Displacement of the plate2 of metering plates of faba bean seeds with (ABS) material
Source: Authors' determination.

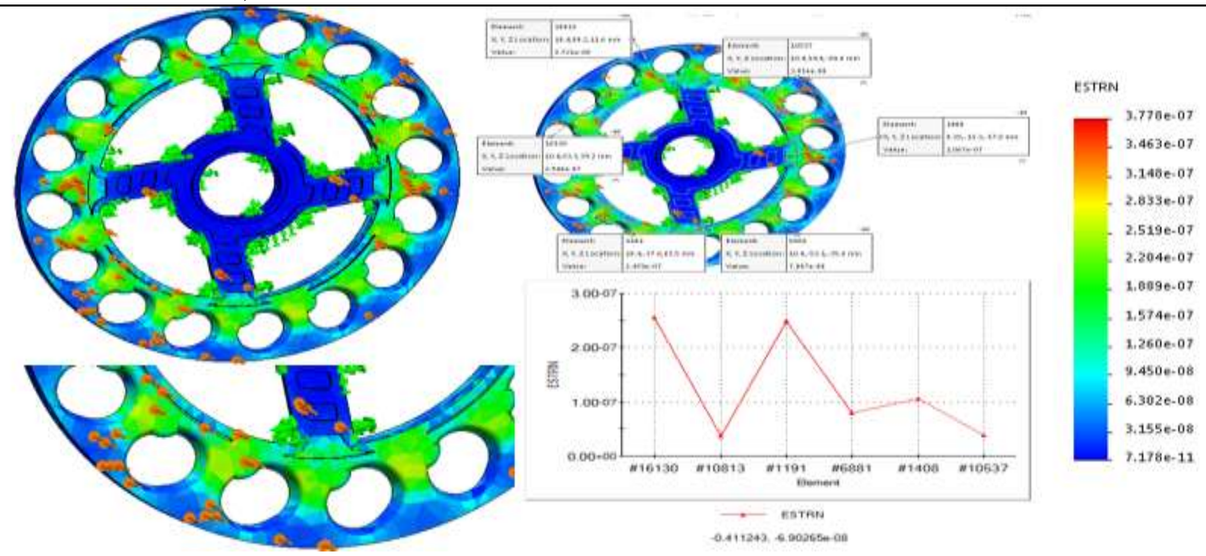

Fig. 29. Strain of the plate 2 of metering plates of faba bean seeds with (ABS) material
Source: Authors' determination.

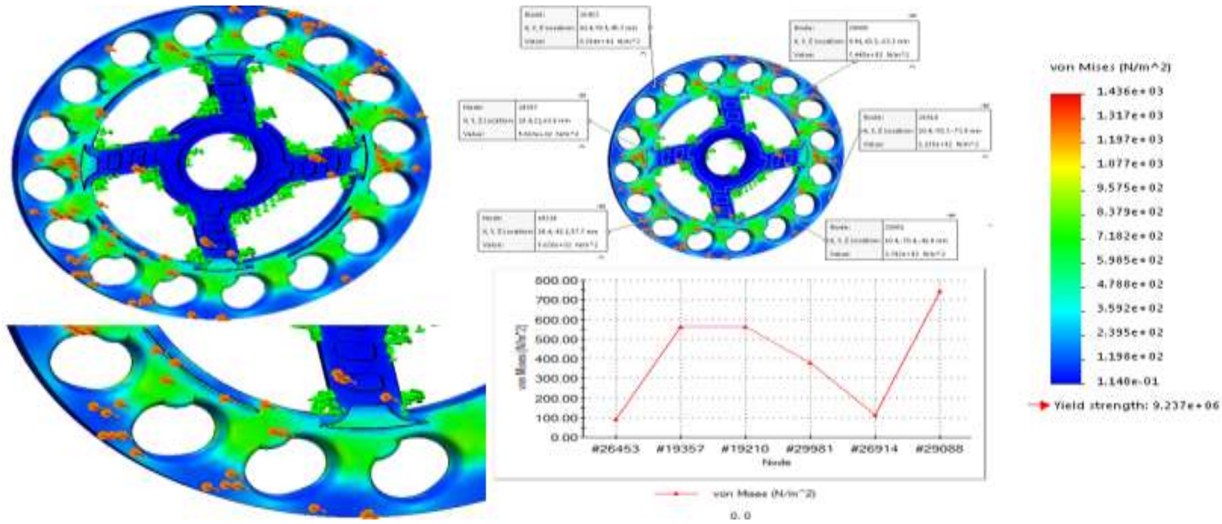

Fig. 30. Stress of the plate 2 of metering plates of faba bean seeds with (TPU) material
Source: Authors' determination.

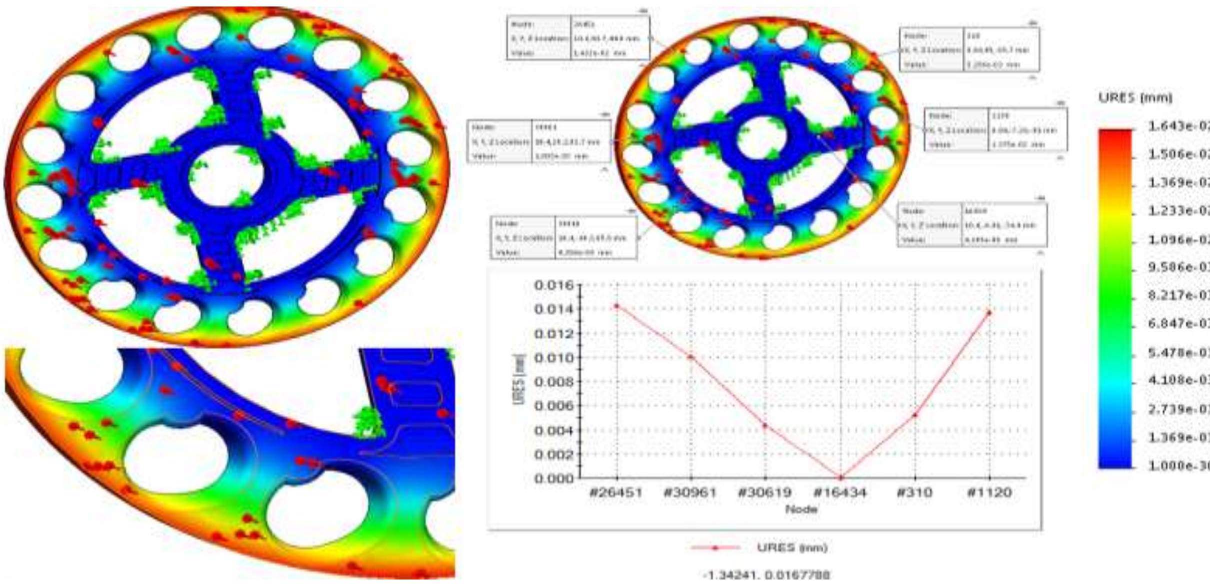

Fig. 31. Displacement of the plate 2 of metering plates of faba bean seeds with (TPU) material
Source: Authors' determination.

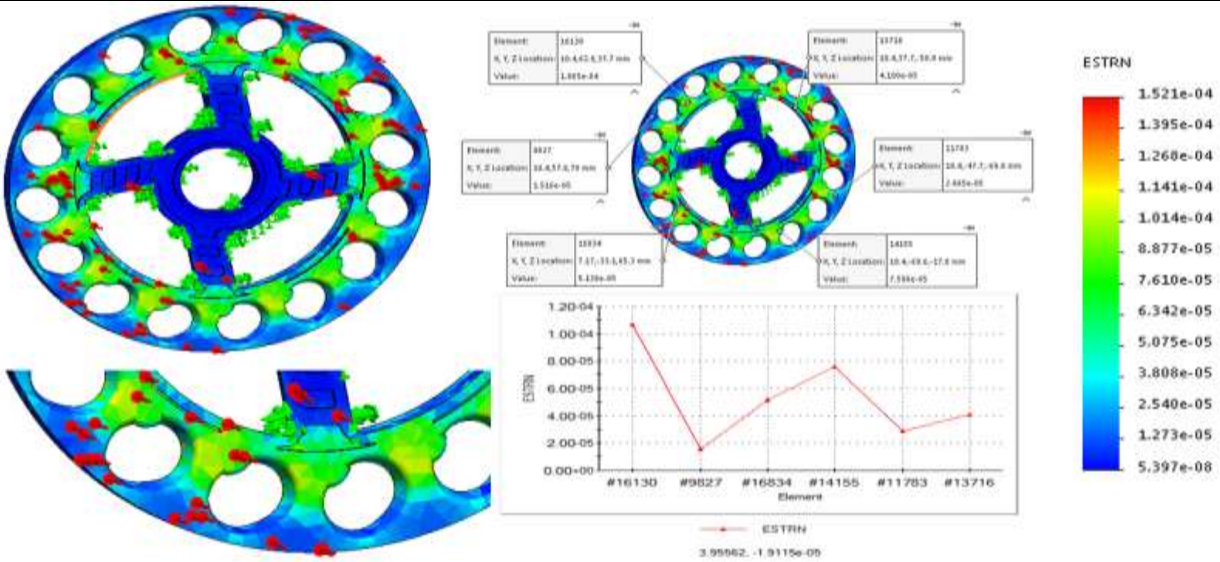

Fig. 32. Strain of the plate 2 of metering plates of faba bean seeds with (TPU) material
Source: Authors' determination.

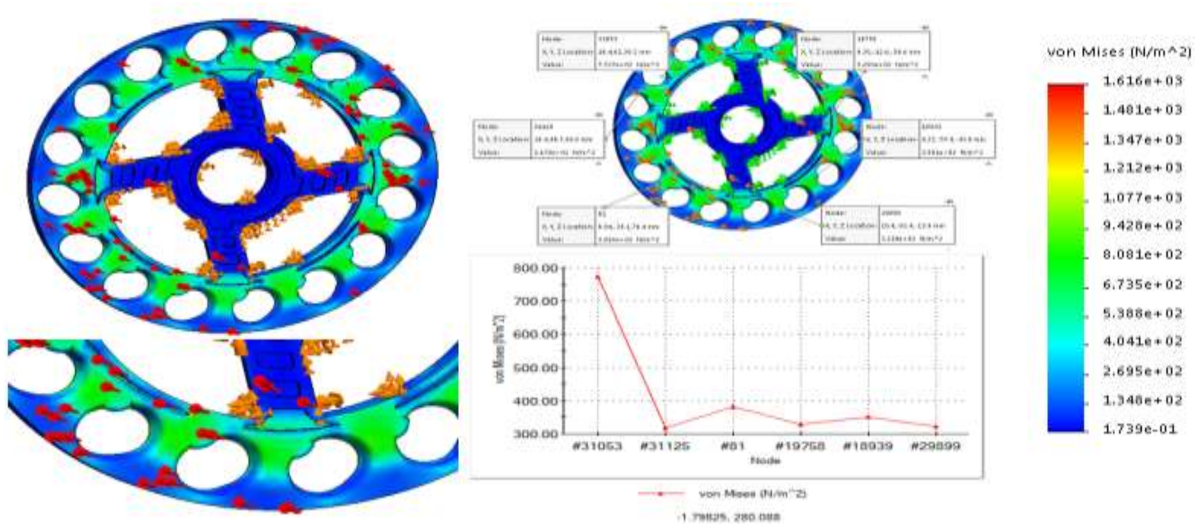

Fig. 33. Stress of the plate 2 of metering plates of faba bean seeds with (NYLON) material
Source: Authors' determination.

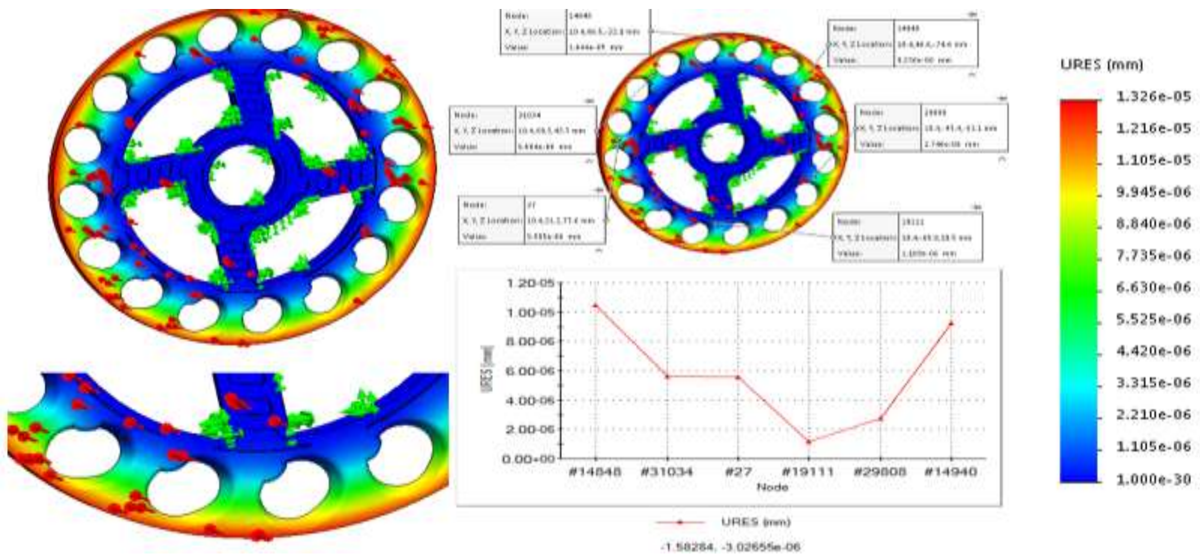

Fig. 34. Displacement of the plate 2 of metering plates of faba bean seeds with (NYLON) material
Source: Authors' determination.

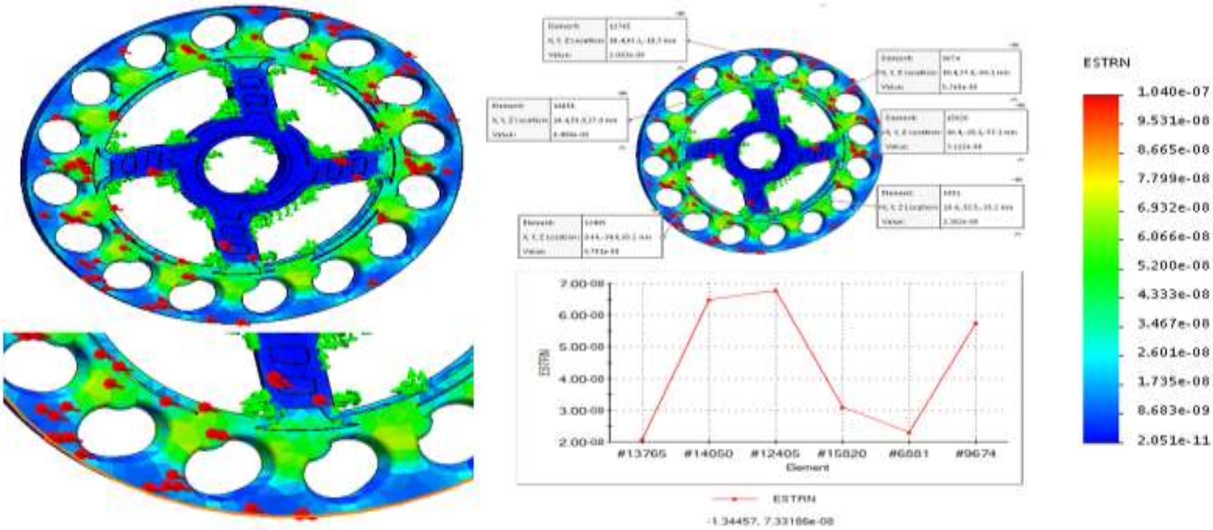

Fig. 35. Strain of the plate 2 of metering plates of faba bean seeds with (NYLON) material
Source: Authors' determination.

❖ Faba Bean plates (plate 3)

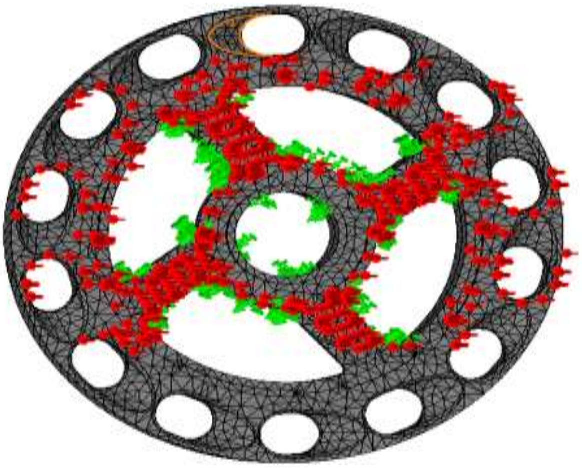

Study name	Static (shape3) (-Default-)
Mesh type	Solid Mesh
Mesher Used	Standard mesh
Automatic Transition	Off
Include Mesh Auto Loops	Off
Jacobian points	4 points
Element size	4.51056 mm
Tolerance	0.225528 mm
Mesh quality	High
Total nodes	31993
Total elements	17335
Maximum Aspect Ratio	16.308
Percentage of elements with Aspect Ratio < 3	76.8
Percentage of elements with Aspect Ratio > 10	0.496
% of distorted elements (Jacobian)	0
Time to complete mesh(hh:mm:ss)	00:00:22
Computer name	DELL-PC

Fig. 36. Mesh generation of plate 1 (Total number of nodes 31993)
Source: Authors' determination.

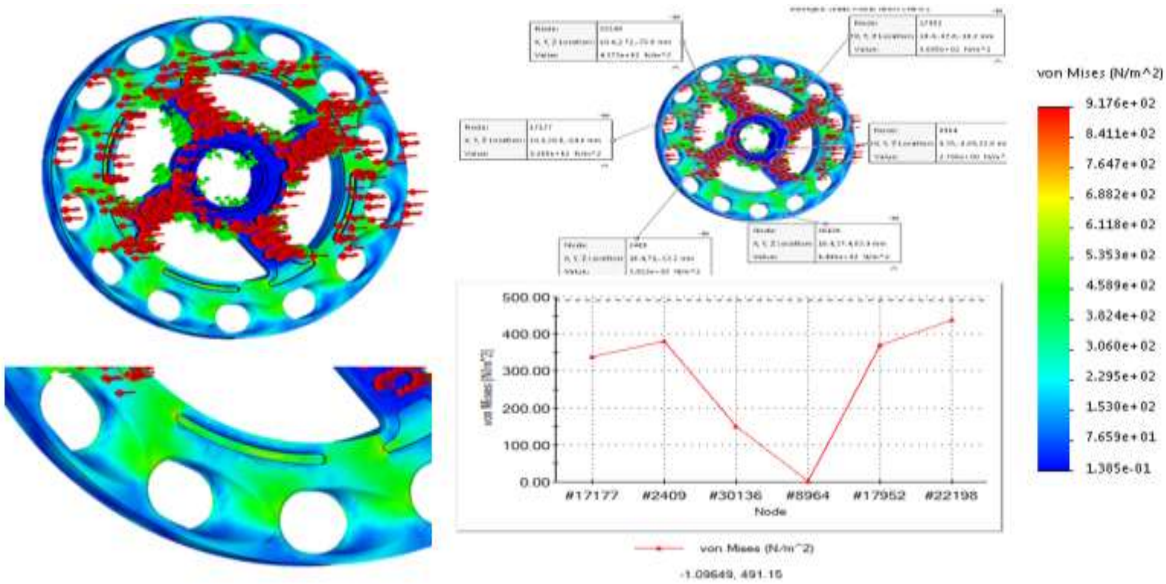

Fig. 37. Stress of the Plate 3 of metering plates of faba bean seeds with (PA) material
Source: Authors' determination.

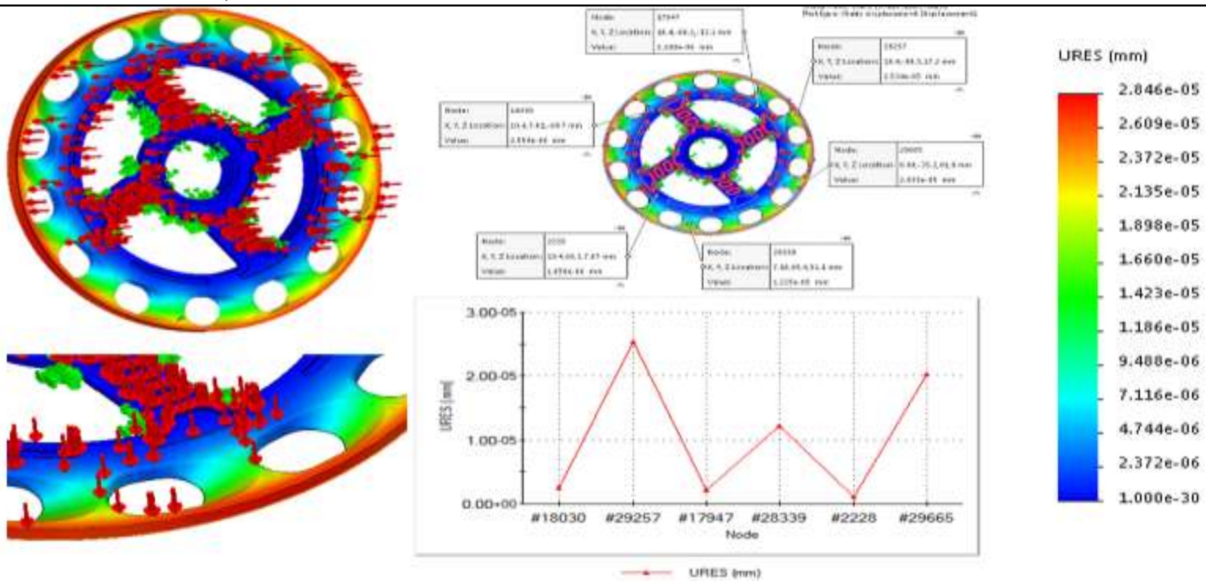

Fig. 38. Displacement of the Plate3 of metering plates of faba bean seeds with (PA) material
Source: Authors' determination.

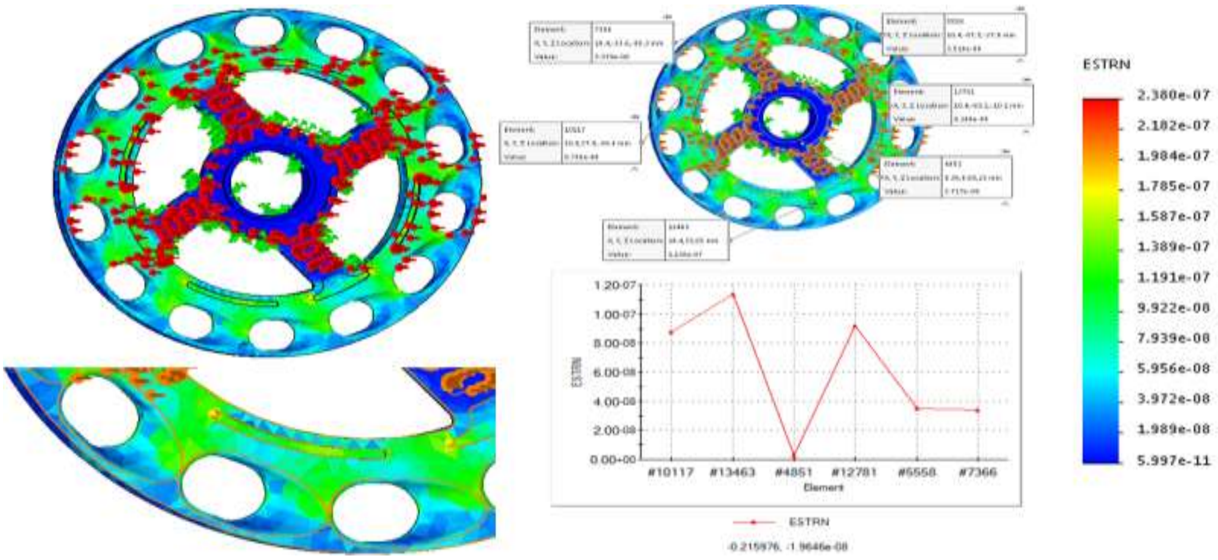

Fig. 39. Strain of the Plate 3 of metering plates of faba bean seeds with (PA) material
Source: Authors' determination.

CONCLUSIONS

Faba bean metering plates with dimensions of 18.5 cm and a thickness of 6.4 mm were developed and made using a 3D printer and the Solidworks software version 2018.

ABS, TPU, NYLON, and PA were used as fabrication materials for printing the metering plates and were then analyzed.

Plate 1 (TPU) had a maximum stress of 1.600e+04 N/m^2 and a minimum stress of 1.572e-02 N/m^2.

When the maximum strain and safety factor were 1.929e-03 and 5.874e+08, respectively, displacement was 1.596e-01 mm.

The minimum strain and safety factor were 3.109e-07 and 5.775e+02, respectively.

The average elongation, projected area, flatness, and roundness were all calculated. Geometric Mean Diameter of the Plate 1 was (1.26, 117.81, 2.61, 0.789, 1.76 and 12.25) correspondingly. In ideal situations, it is recommended to use Panel 1 made of TPU.

REFERENCES

[1]Adewale, B. D., O. B, Kehinde., Aremu, C. O., Popoola, J. O., Dumet, D. J., 2010, Seed metrics for genetic and shape determinations in African yam bean (Sphenostylis stenocarpa Hochst. Ex. A. Rich.) harms, African Journal of Plant Science, Vol. 4(4), 107–11, Accessed on 10/11/2022.

[2]Çetin, N., 2022, Machine learning for varietal binary classification of soybean (Glycine max (L.) Merrill) seeds based on shape and size attributes. Food Analytical Methods, 1-14. Accessed on 10/11/2022.
[3]Cervantes, E., Martín, J. J., Saadaoui, E., 2016, Updated methods for seed shape analysis. Scientifica. Accessed on 10/11/2022.
[4]Cervantes, E., Saadaoui, E., Tocino, Á., Gómez, J. J. M., 2019, Seed shape quantification in the model legumes: Methods and applications. The Model Legume Medicago truncatula, 92-98. Accessed on 10/11/2022.
[5] Cervantes, E., Mart´ın Javier, J., Ardanuy, R., de Diego, J. G., Tocino, A., 2010, Modeling the Arabidopsis seed shape by a cardioid: ´ efficacy of the adjustment with a scale change with factor equal to the Golden Ratio and analysis of seed shape in ethylene mutants," Journal of Plant Physiology, Vol. 167(5), 408– 410, Accessed on 10/11/2022.
[6]Daniel, I. O., Oduwaye, O. O., Porbeni, J., 2012, Digital seed morpho-metric characterization of tropical maize inbred lines for cultivar discrimination," International Journal of Plant Breeding and Genetics, Vol. 6(4), 245–251, Accessed on 10/11/2022.
[7]Fıratlıgil-Durmuş, E., Šárka, E., Bubník, Z., Schejbal, M., Kadlec, P., 2010, Size properties of legume seeds of different varieties using image analysis. Journal of Food Engineering, 99(4), 445-451.
[8]He, C., Zeng, W., Kong, R., Gong, J., Ma, W., Tie, Q., ... Guan, J., 2021, Design, Preparation, and Mechanical Property Study of Polylactic Acid/Ca2BO3Cl: Eu2+, Dy3+ Composite Material for 3D Printing. 3D Printing and Additive Manufacturing. Accessed on 10/11/2022.
[9] Ibrahim, E. J., Liao, Q., Wang, L., Liao, Y., Yao, L., 2018, Design and experiment of multi-row pneumatic precision metering device for rapeseed. International Journal (Agricultural and Biological Engineering), 11(5), 116-123. Accessed on 10/11/2022.
[10]Júnior, P. A., Correa, P. C., Pinto, F. A. C., Queiroz, D. M., 2007, Aerodynamic properties of coffee cherries and beans. Biosystems Engineering, 98(1), 39-46. Accessed on 10/11/2022.
[11]Lazari, G., Couvreur, P., Mura, S., (2017), Multicellular tumour spheroids: a relevant 3D model for the in vitro preclinical investigation of polymer Nano medicines. Polymer Chemistry, 8(34), 4947-4969. Accessed on 10/11/2022.
[12]Martın-Gomez, J.J., Tocino, A., Ardanuy, R. et al., 2014, Dynamic analysis of Arabidopsis seed shape reveals differences in cellulose mutants. Acta Physiologiae Plantarum 36: 1585–1592. Accessed on 10/11/2022.
[13]Martín-Gómez, J. J., Del Pozo, D. G., Tocino, A.,... Cervantes, E., 2021, Geometric models for seed shape description and quantification in the Cactaceae. Plants, 10(11), 2546. Accessed on 10/11/2022.
[14]Mohd Aras, M. S., Md Zain, Z., Kamaruzaman, A. F., Ab Rashid, M. Z., Ahmad, A., Mohd Shah, H. N., ... AbAzis, F., 2021, Design and development of remotely operated pipeline inspection robot. In Proceedings of the 11th National Technical Seminar on Unmanned System Technology 2019 (pp. 15-23). Springer, Singapore. Accessed on 10/11/2022.
[15]Nikolay, Z., Nikolay, K., Gao, X., Li, Q. W., Mi, G. P., Huang, Y. X., 2022, Design and testing of novel seed miss prevention system for single seed precision metering devices. Computers, Electronics in Agriculture, 198, 107048. Accessed on 10/11/2022.
[16]Ozkan, G., Koyuncu, M. A., 2005, Physical and chemical composition of some walnut (Juglansregia L) genotypes grown in Turkey. Grasas y Aceites, 56(2), 141-146. Accessed on 10/11/2022.
[17]Rodríguez-Lorenzo, J. L., Martín-Gómez, J. J., Tocino, Á., Juan, A., Janoušek, B., Cervantes, E., 2022, New geometric models for shape quantification of the dorsal view in seeds of Silene species. Plants, 11(7), 958. Accessed on 10/11/2022.
[18]Sayıncı, B., Ercişli, S., Akbulut, M., Şavşatlı, Baykal, Y., H., 2015, Determination of shape in fruits of cherry laurel (Prunus laurocerasus) accessions by using Elliptic Fourier analysis. Accessed on 10/11/2022.
[19]Segalman, D., Reese, G., Field Jr, R., Fulcher, C., 2000, Estimating the probability distribution of von Mises stress for structures undergoing random excitation. J. Vib. Acoust., 122(1), 42-48. Accessed on 10/11/2022.
[20]Sharma, A., Chhabra, D., Sahdev, R., Kaushik, A., Punia, U., 2022, Investigation of wear rate of FDM printed TPU, ASA and multi-material parts using heuristic GANN tool. Materials Today: Proceedings. Accessed on 10/11/2022.
[21]Shi, L., Wu, J., Sun, W., Zhang, F., Sun, B., Liu, Q., Zhao, W., 2014, Transactions of the Chinese Society of Agricultural Engineering ,Simulation test for metering process of horizontal disc precision metering device based on discrete element method., 30(8), 40-48. Accessed on 10/11/2022
[22] Simo, J. C, Fox, D. D., 1989, On a stress resultant geometrically exact shell model. Part I: Formulation and optimal parametrization. Computer Methods in Applied Mechanics and Engineering, 72(3), 267-304. Accessed on 10/11/2022.
[23]Vishwakarma, S. K., Pandey, P., Gupta, N. K., 2017, Characterization of ABS material: a review. Journal of Research in Mechanical Engineering, 3(5), 13-16. Accessed on 10/8/2022
[24]Williams, K., Munkvold, J., Sorrells, M., 2013, Comparison of digital image analysis using elliptic Fourier descriptors and major dimensions to phenotype seed shape in hexaploid wheat (Triticumaestivum L.), Euphytica, Vol. 190(1), 99–116. Accessed on 10/11/2022.
[25]Xie, C., Zhang, D., Yang, L., Cui, T., Yu, T., Wang, D., Xiao, T., 2021, Experimental analysis on the variation law of sensor monitoring accuracy under different seeding speed and seeding spacing. Electronics and Computers in Agriculture, 189, 106369. Accessed on 10/11/2022
[26]Yang, L., Zhang, D., Xie, C., Cui, T., Yu, T., Wang, D., Xiao, T., 2021, Experimental analysis on the variation law of sensor monitoring accuracy under different seeding speed and seeding spacing.

Electronics in Agriculture, 189, 106369. Accessed on 10/8/2022

[27]Zhang, M., Zeng, W., Lei, Y., Chen, X., Zhang, M., Li, C., Qin, S., 2022. A novel sustainable luminescent ABS composite material for 3D printing. European Polymer Journal, 111406. Accessed on 10/11/2022.

[28]Zhuang, Y., Song, W., Ning, G., Sun, X., Sun, Z., Xu, G., ... Tao, S., 2017, 3D–printing of materials with anisotropic heat distribution using conductive polylactic acid composites. Materials & Design, 126, 135-140. Accessed on 10/11/2022.